

Enhanced Piezoelectric Property of Barium Titanate Single Crystals with Engineered Domain Configurations

Satoshi WADA*, Shingo SUZUKI, Tatsuo NOMA, Takeyuki SUZUKI, Minoru OSADA¹, Masato KAKIHANA², Seung-Eek PARK³, L. Eric CROSS³ and Thomas R. SHROUT³

Department of Applied Chemistry, Tokyo University of Agriculture & Technology, 24-16 Nakamachi 2-chome, Koganei, Tokyo 184-8588, Japan

¹Institute of Physical & Chemical Research, 2-1 Hirosawa, Wako, Saitama 351-0198, Japan

²Materials & Structures Laboratory, Tokyo Institute of Technology, 4259 Nagatsuta-cho, Midori-ku, Yokohama 226-8502, Japan

³Materials Research Laboratory, Pennsylvania State University, University Park, PA 16802, U.S.A.

(Received May 10, 1999; accepted for publication June 18, 1999)

Piezoelectric properties of barium titanate single crystals were investigated at room temperature as a function of crystallographic orientation. When a unipolar electric field was applied along [001], its strain vs electric-field curve showed a large hysteresis, and finally barium titanate crystal became to single-domain state with piezoelectric constant d_{33} of 125 pC/N over 20 kV/cm. On the other hand, electric-field exposure below 6 kV/cm along [111] resulted in a high d_{33} of 203 pC/N and a hysteresis-free strain vs electric-field behavior, which suggested the formation of an engineered domain configuration in a tetragonal barium titanate crystal. Moreover, when an electric field over 6 kV/cm was applied along [111], two discontinuous changes were observed in its strain vs electric-field curve. *In situ* domain observation and Raman measurement under an electric field suggested an electric-field-induced phase transition from tetragonal to monoclinic at around 10 kV/cm, and that from monoclinic to rhombohedral at around 30 kV/cm. Moreover, in a monoclinic barium titanate crystal, electric-field exposure along [111] resulted in the formation of another new engineered domain configuration with d_{33} of 295 pC/N.

KEYWORDS: engineered domain configuration, piezoelectric property, barium titanate single crystal, *in situ* domain observation, *in situ* Raman measurement, crystallographic orientation, electric-field induced phase transition

1. Introduction

Recently, in [001] oriented rhombohedral $\text{Pb}(\text{Zn}_{1/3}\text{Nb}_{2/3})\text{O}_3\text{-PbTiO}_3$ (PZN-PT) single crystals, ultrahigh piezoelectric activities were found by Park *et al.*¹⁾ and Park and ShROUT,²⁻⁴⁾ with strain over 1.7%, piezoelectric constant d_{33} over 2500 pC/N, electromechanical coupling factor k_{33} over 90% and hysteresis-free strain vs electric-field behavior. $(1-x)\text{PZN}-x\text{PT}$ single crystals with $x < 0.09$ have rhombohedral $3m$ symmetry at room temperature, and their polar directions are $\langle 111 \rangle$.^{5,6)} However, unipolar electric-field exposure along the [111] direction showed a large hysteretic strain vs electric-field behavior and a low d_{33} below 100 pC/N. On the other hand, unipolar electric-field exposure along the [001] direction exhibited non-hysteretic strain vs electric-field behavior and d_{33} over 2500 pC/N in 0.92PZN-0.08PT crystals. To explain the above strong anisotropy in piezoelectric properties, *in situ* domain observation was done using [111] and [001] oriented pure PZN and 0.92PZN-0.08PT single crystals.^{7,8)} As a result, when electric field was applied along the [001] direction, a very stable domain structure appeared under 0.2 kV/cm, and domain wall motion was undetectable under DC-bias of up to 20 kV/cm, resulting in hysteresis-minimized strain vs electric-field behavior.

Figure 1 shows a schematic domain configuration for [001] poled rhombohedral $3m$ crystals. [001] poled $3m$ crystals must have four domains with four equivalent polar vectors along [111], $[\bar{1}\bar{1}\bar{1}]$, $[1\bar{1}\bar{1}]$ and $[\bar{1}\bar{1}1]$ directions because of their polar directions of $\langle 111 \rangle$. Therefore, the component of each polar vector along the [001] direction is completely equal each other, so that each domain wall cannot move under electric-field exposure along the [001] direction owing to the equivalent domain wall energies.²⁻⁴⁾ This suggests the possibility of controlling domain configuration in single crys-

tals using crystallographic orientation, and the appearance of a new technology in domain engineering field, as well as a conventional constraint of domain wall motion by acceptor dopants, i.e., “Hard” PZT. Thus, this special domain structure in single crystals (Fig. 1) using crystallographic orientation was called an engineered domain configuration.^{2-4,7,8)}

The engineered domain configuration is expected to possess the following three features for piezoelectric performance: (1) hysteresis-free strain vs electric-field behavior owing to inhibition of domain wall motion, (2) higher piezoelec-

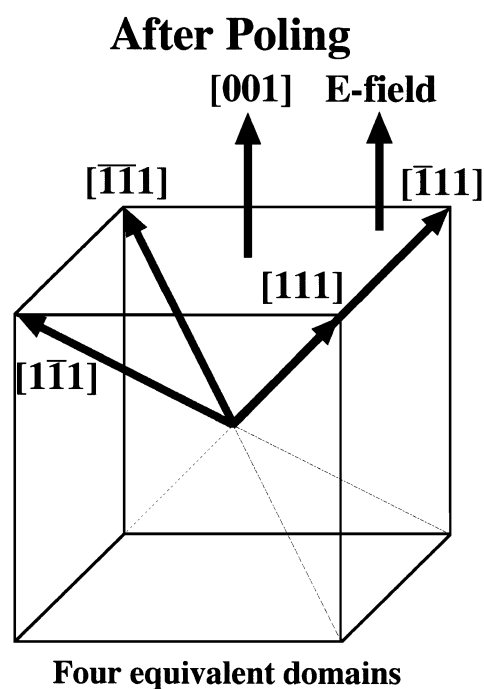


Fig. 1. Schematic domain configuration for [001] poled rhombohedral $3m$ crystal.

*E-mail address: swada@cc.tuat.ac.jp

tric constant along the non-polar direction than that along the polar direction and (3) change of macroscopic symmetry in crystals with engineered domain configuration.^{7,8)} Therefore, if the concept of the engineered domain configuration can be applied to other ferroelectric single crystals, enhanced piezoelectric properties are expected. In this study, a barium titanate (BaTiO_3) single crystal was chosen for the first step in the application of the engineered domain configuration. This is because BaTiO_3 single crystal is one of the well-studied ferroelectrics, a typical non-lead ferroelectric, and a perovskite-type structure similar to PZN and PZN-PT.

In this study, the piezoelectric properties of BaTiO_3 single crystals were investigated at room temperature as a function of crystallographic orientation, such as [001] and [111] directions. Their domain configurations were also observed as a function of electric field and crystallographic orientation using a polarizing microscope. The behavior of domain wall motion will be discussed in relation to the observed strain vs electric-field behavior. Moreover, *in situ* Raman measurement was done to study changes in crystal symmetry as a function of electric field and crystallographic orientation.

2. Experimental

2.1 Sample

BaTiO_3 single crystals were prepared by a top-seeded solution growth (TSSG) method at Fujikura, Ltd. In TSSG-grown BaTiO_3 crystals, the concentration of most impurities (Cr, Mn, Fe, Co, Ni, Cu) was below 2–3 ppm.^{9,10)} Optically, BaTiO_3 crystals were transparent and light yellow. The details of preparation of BaTiO_3 single crystals and their characterization were described elsewhere.^{9–12)} These crystals were oriented along [001] and [111] directions using the back-reflection Laue method. All characterizations and treatments were done at Fujikura, Ltd.

2.2 Measurement of piezoelectric property

For electrical measurement of BaTiO_3 crystals, samples were prepared by polishing to achieve flat and parallel surfaces onto which gold electrodes were sputtered. Prior to piezoelectric measurements, dielectric properties were measured with a LCR meter (Hewlett-Packard 4263A) at room temperature, and it was confirmed that their dielectric loss was below 0.1% at 100 Hz. High electric field measurements included polarization and strain using a modified Sawyer-Tower circuit and a linear variable differential transducer (LVDT) driven by a lock-in amplifier (Stanford Res. Sys., model SR830). Electric fields were applied using an amplified triangular waveform at 0.1 Hz, using a Kepco BOP-1000M high-voltage DC amplifier (<1 kV) and a Trek 609C-6 high-voltage DC amplifier (≥ 1 kV).

2.3 *In situ* domain observation and *in situ* Raman measurement

For *in situ* domain observation and Raman measurement under DC-bias, samples were prepared by polishing to an optimum size of approximately $0.2 \times 0.5 \times 4 \text{ mm}^3$. Their top and bottom surfaces ($0.5 \times 4 \text{ mm}^2$) were mirror-polished, normal to an incident light. Gold electrodes were sputtered on both sides ($0.2 \times 4 \text{ mm}^2$), and the width between electrodes was around 0.5 mm along the [001] or [111] direction. The details were described elsewhere.^{7,8,13)} Domain configuration was

always observed under crossed-nicols using a polarizing microscope (Olympus, BX50-31P). DC-bias exposure was done along the [001] or [111] direction, being normal to the incident polarized light, using a Trek 610D high-voltage DC amplifier. Raman spectra under DC-bias were measured in the backward scattering geometry using a Raman scattering spectrometer with a triple monochromator (Jobin-Yvon, T64000). DC-bias exposure was done in the same way as that in domain observation. The top surface ($0.5 \times 4 \text{ mm}^2$) was excited by unpolarized Ar ion laser with a wavelength of 514.5 nm and power below 20 W/cm^2 . The details are described elsewhere.¹⁴⁾

3. Results and Discussion

3.1 [001] oriented BaTiO_3 single crystals

Figure 2 shows a strain vs electric-field curve of a [001] oriented BaTiO_3 crystal measured using a unipolar electric field with 0.1 Hz at 25°C. It should be noted that this curve was not obtained at the 1st cycle of electric-field exposure, but after the 2nd cycle of electric-field exposure, i.e., this strain behavior means that after poling. The strain behavior in [001] oriented BaTiO_3 crystal exhibits a large strain of around 1% and a remarkable hysteresis. Such a large strain of around 1% caused by tetragonality of BaTiO_3 , $c/a \sim 1.011$, which suggests that domain reorientation can contribute significantly to strain behavior. Moreover, at high electric field above 20 kV/cm, the apparent d_{33} was directly estimated at 125 pC/N from Fig. 2. This value was close to $d_{33} \sim 90 \text{ pC/N}$ in the single-domain BaTiO_3 crystal reported by Zgonik *et al.*,¹⁵⁾ which indicated that over 20 kV/cm, BaTiO_3 crystal might be single-domain state. Therefore, Fig. 2 suggests that domain wall motion can affect largely strain behavior in [001] oriented BaTiO_3 crystal.

Figure 3 shows the results of *in situ* domain observation under DC-bias below 22.1 kV/cm in a [001] oriented BaTiO_3 crystal. The results in Fig. 3 was also obtained after the 2nd cycle of electric-field exposure, and thus indicates that domain configuration in Fig. 3(a) was domain configuration without DC-bias after poling at 22.1 kV/cm. Figure 3(a) shows systematic domain configuration with $90^\circ W_f$ domain

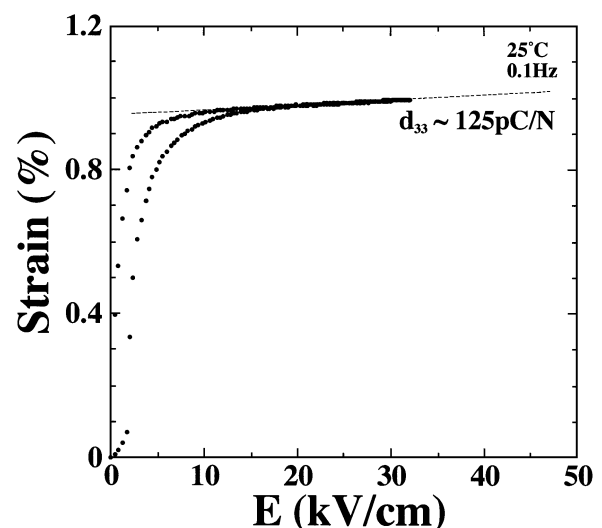


Fig. 2. Strain vs electric-field curve for [001] oriented BaTiO_3 crystal under unipolar electric field below 35 kV/cm with 0.1 Hz at 25°C.

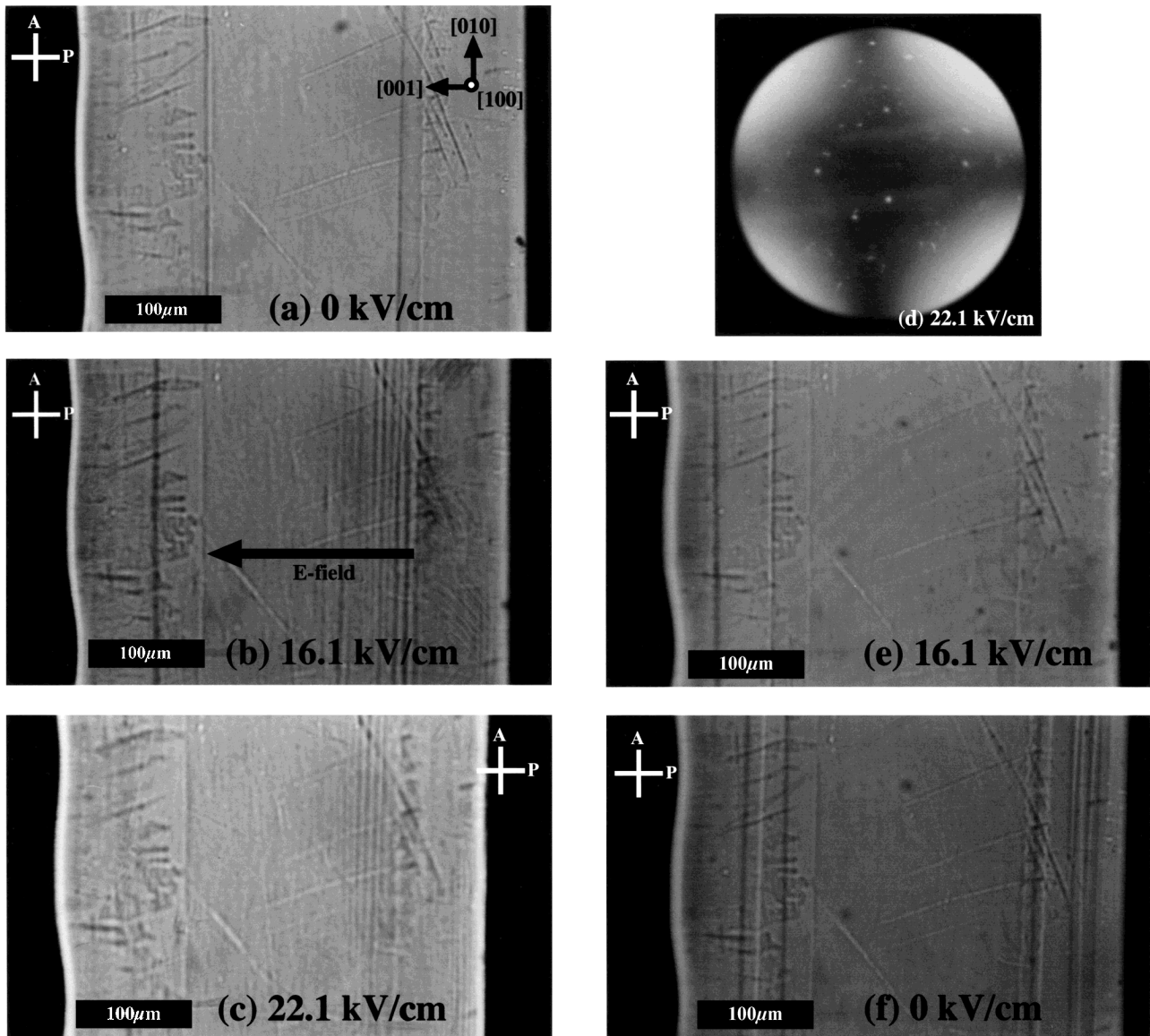


Fig. 3. *In situ* domain observation at various electric fields below 22.1 kV/cm in [001] oriented BaTiO₃ crystal.

walls of {101} planes.¹⁶⁾ With increasing electric field, domain wall motion was observed below 1 kV/cm, and finally at around 22.1 kV/cm, an almost single-domain state was achieved, except near the surface, as shown in Fig. 3(c). Moreover, a conoscopic figure (Fig. 3(d)) in the same region as that of Fig. 3(c) corresponded to a uniaxial flush interference figure, which can be given under a conoscope when the optic axis of uniaxial crystals, the [001] direction in a tetragonal BaTiO₃ crystal, is parallel to a microscopic stage.¹⁷⁾ This means that at 22.1 kV/cm, most of the crystal was transformed to the single-domain state.

On the other hand, with decreasing electric field from 22.1 kV/cm, new domains appeared and domain wall density increased (Figs. 3(e) and 3(f)). However, domain wall density at decrease of electric field was less than that at increase of electric field, even if the electric fields had the same values, *e.g.*, a comparison between Figs. 3(b) and 3(e). This revealed that a difference in the domain wall density at increasing and decreasing electric fields caused the large hysteresis in the strain vs electric-field curve (Fig. 2).

3.2 [111] oriented BaTiO₃ single crystals

Strain vs electric-field behaviors in [111] oriented BaTiO₃ single crystals were very complicated, as shown in Figs. 4–6. All these curves were also obtained after the 2nd cycle of electric-field exposure, *i.e.*, these strain behaviors represent those after poling. To simplify the complicated phenomena, these strain vs electric-field behaviors were separated into four regions: (1) low electric field under 5 kV/cm, (2) middle electric field from 5 to 16 kV/cm, (3) high electric field from 16 to 26 kV/cm and (4) ultrahigh electric field above 26 kV/cm, and each behavior is discussed.

3.2.1 Low electric-field region under 5 kV/cm

In the low electric-field region as shown in Fig. 4, strain was almost proportional to electric field without hysteresis. In tetragonal BaTiO₃, the coercive electric field E_c was reported to be around 1 kV/cm,¹⁸⁾ and in this study, domain wall motion in [001] oriented BaTiO₃ crystals was observed below 1 kV/cm (Fig. 3). Thus, the strain behavior in Fig. 4 suggested that the engineered domain configuration shown in Fig. 7 was induced in [111] poled tetragonal BaTiO₃ crystals. Moreover,

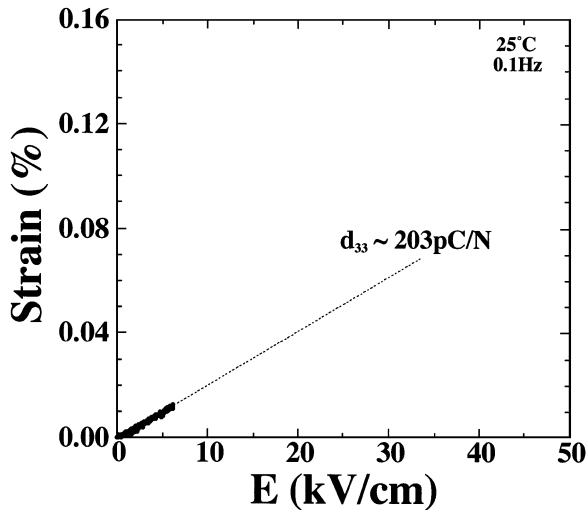


Fig. 4. Strain vs electric-field curve for [111] oriented BaTiO₃ crystal under unipolar electric field below 5 kV/cm with 0.1 Hz at 25°C.

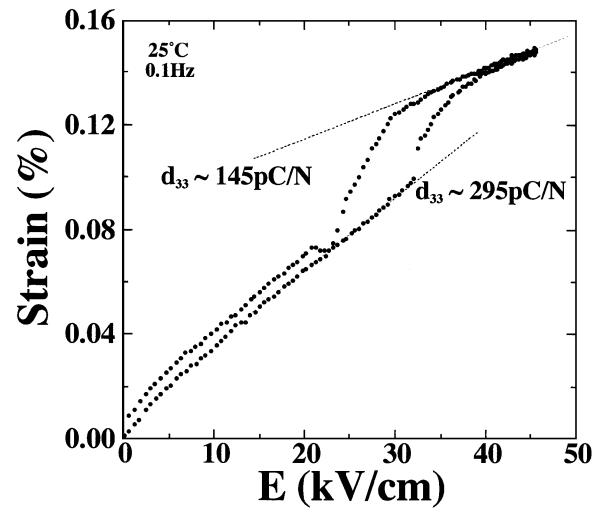


Fig. 6. Strain vs electric-field curve for [111] oriented BaTiO₃ crystal under unipolar electric field below 45 kV/cm with 0.1 Hz at 25°C.

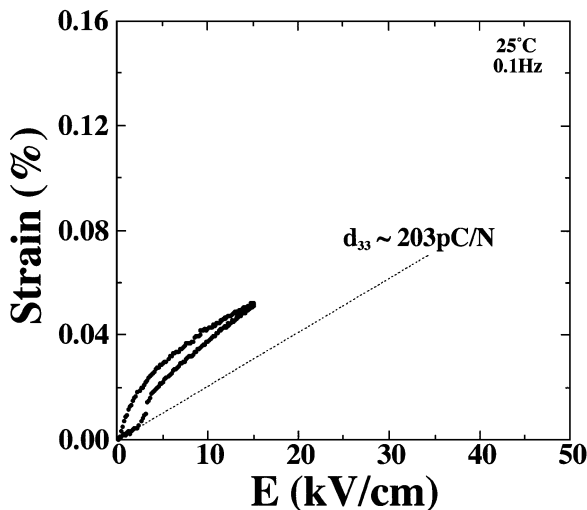


Fig. 5. Strain vs electric-field curve for [111] oriented BaTiO₃ crystal under unipolar electric field below 16 kV/cm with 0.1 Hz at 25°C.

the apparent d_{33} obtained directly from Fig. 4 was 203 pC/N, which was almost 1.6 times higher than that in a [001] poled single-domain BaTiO₃ crystal.

To confirm the formation of the engineered domain configuration, *in situ* domain observation in [111] oriented tetragonal BaTiO₃ crystals was done below 5 kV/cm. Figure 8 shows the domain configuration at various electric fields below 3.8 kV/cm. The domain structure under no DC-bias was highly systematic, and three ferroelectric domains with polar directions of [100], [010] and [001] were observed, as shown in Fig. 8(a). Although the electric field increased to 3.8 kV/cm, the domain structure did not change, except near the surface. This domain configuration was almost the same as the expected one in Fig. 7. Thus, we confirmed the formation of the engineered domain configuration in [111] poled tetragonal BaTiO₃ crystals.

The above results indicate that application of the engineered domain configuration to tetragonal BaTiO₃ crystals resulted in enhanced piezoelectric activities, *i.e.*, higher d_{33} and non-hysteretic strain vs electric-field behavior. Therefore, we believe that the concept of the engineered domain configura-

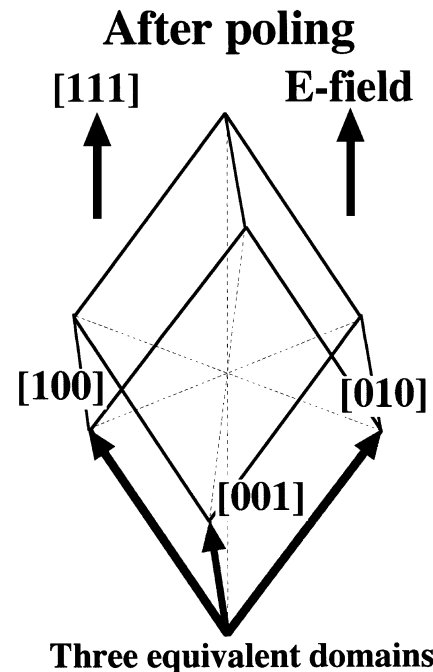


Fig. 7. Schematic engineered domain configuration for [111] poled tetragonal $4mm$ BaTiO₃ crystal.

tion is universal, and can apply to all perovskite-type ferroelectric crystals.

3.2.2 Middle electric-field region from 5 to 16 kV/cm

In the middle electric-field region from 5 to 16 kV/cm, a discontinuous change and a large hysteresis were observed, as shown in Fig. 5. In general, a hysteresis in the strain vs electric-field curve suggests the occurrence of domain wall motion or electric-field-induced phase transition. Thus, *in situ* domain observation and *in situ* Raman observation were done in the electric-field region. As a result, with increasing electric field from 6 to 10 kV/cm, domain wall density increased, while with increasing electric field from 10 to 16 kV/cm, domain wall density decreased, and partially single-domain region appeared. Measurement of the extinction position in the observed single-domain region revealed that the regions were assigned to ones with polar directions of $\langle 110 \rangle$. This sug-

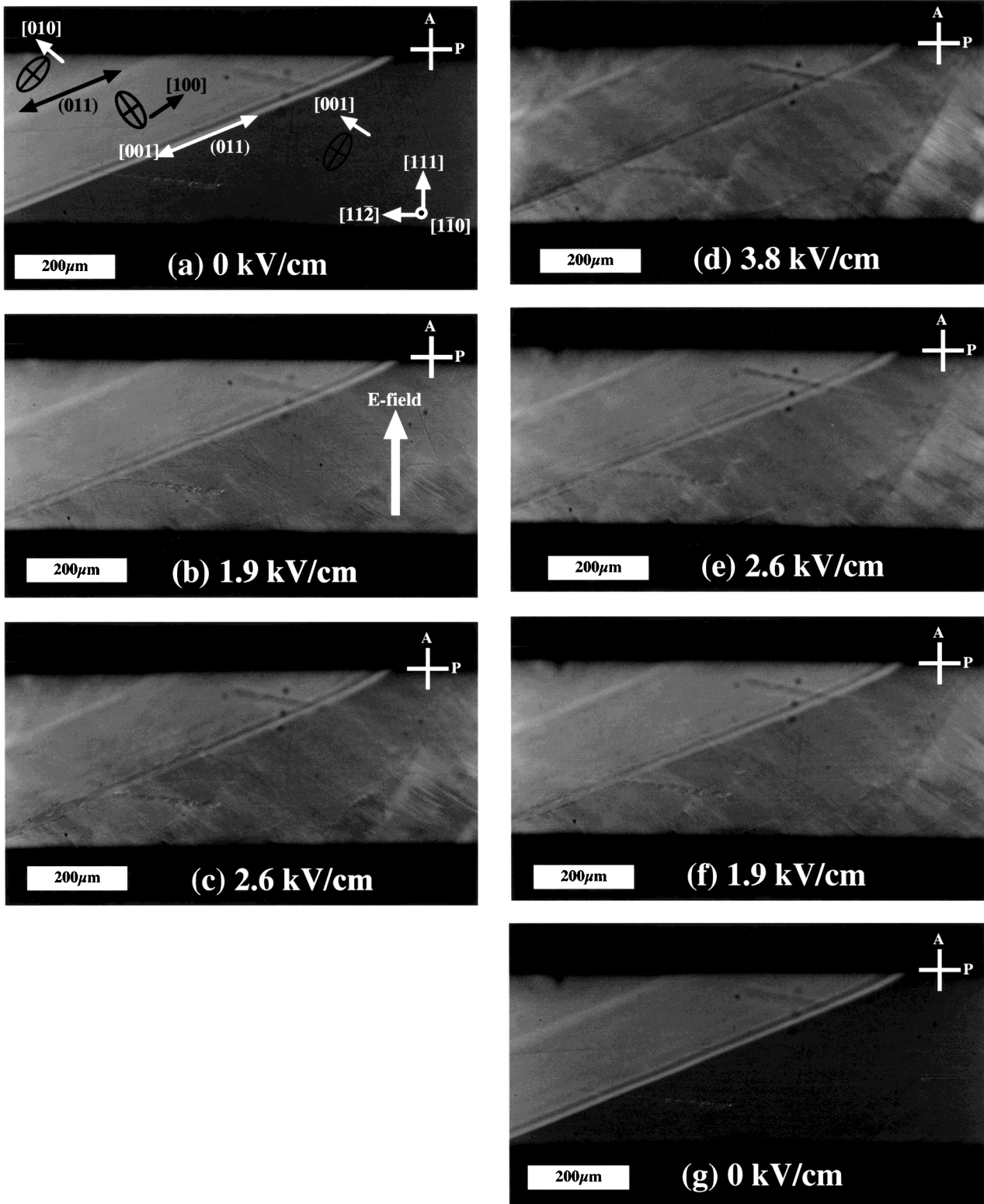


Fig. 8. *In situ* domain observation at various electric fields below 3.8 kV/cm in [111] oriented BaTiO₃ crystal.

gests the formation of monoclinic (=orthorhombic) *m* phase in tetragonal BaTiO₃ crystals. The details are described elsewhere.¹⁴⁾ Moreover, *in situ* Raman measurement was also done in the same electric-field region. As a result, it was found that in electric-field region from 6 to 16 kV/cm, two phases, tetragonal *4mm* and monoclinic *m*, coexisted, and at 16 kV/cm, all regions became to monoclinic *m* phase. The details are also described elsewhere.¹⁴⁾ The above re-

sults suggested that from 6 to 16 kV/cm, an electric-field-induced phase transition occurred from tetragonal to monoclinic phase, which is accompanied by the discontinuous change and large hysteresis as shown in Fig. 5, but more work may be needed.

3.2.3 High electric-field region from 16 to 26 kV/cm

In the high electric-field from 16 to 26 kV/cm, strain was almost proportional to electric field with a non-hysteretic be-

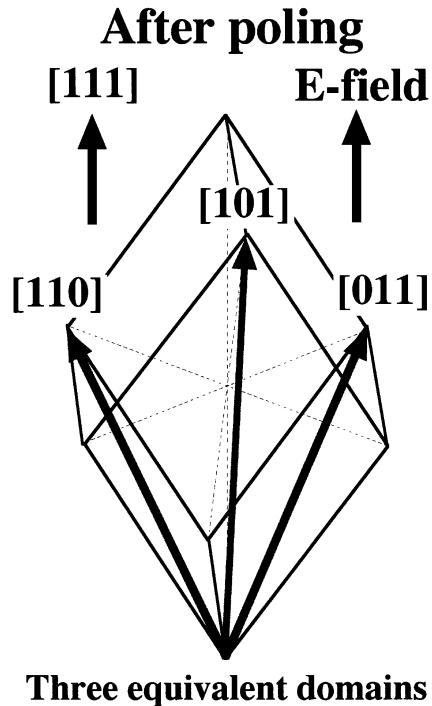


Fig. 9. Schematic engineered domain configuration for [111] poled monoclinic *m* BaTiO₃ crystal.

havior, as shown in Fig. 6. This strain behavior suggested that another engineered domain configuration such as that shown in Fig. 9 can be induced in [111] poled monoclinic BaTiO₃ crystals. Moreover, the apparent d_{33} obtained directly from Fig. 6 was 295 pC/N, which was almost 2.4 times higher than that in a [001] poled single-domain BaTiO₃ crystal. *In situ* Raman measurement in this region revealed that its symmetry was still monoclinic *m*. To confirm the existence of this new engineered domain configuration, *in situ* domain observation in the same electric-field was also done. Figure 10 shows domain configuration at various electric fields from 16.3 to 24.5 kV/cm. Domain walls in Fig. 10(a) appear so complicated, but all domain walls were assigned to 60° and 120° W_f domain walls of {110} and 90° W_f domain walls of {100}.¹⁶⁾ Even if the electric field increased from 16.3 to 24.5 kV/cm, the domain structure did not change, except near the surface. This domain configuration was almost the same as the expected one in Fig. 9. Thus, we confirmed a formation of another new engineered domain configuration in [111] poled monoclinic BaTiO₃ crystals and its enhanced piezoelectric property.

However, based on our expectation regarding the three effects of the engineered domain configuration on piezoelectric performance, as described in *Introduction*, we cannot explain why [111] poled monoclinic BaTiO₃ crystals with the engineered domain configuration (Fig. 9) have 1.5 times higher d_{33} than [111] poled tetragonal BaTiO₃ crystals with the engineered domain configuration (Fig. 7). This difference should be explained on the basis of crystallographic approach, as will be described elsewhere.¹⁴⁾

3.2.4 Ultrahigh electric-field region above 26 kV/cm

In the ultrahigh electric-field region above 26 kV/cm, a discontinuous change and a large hysteresis were observed in Fig. 6. To clarify the origin of this discontinuous change,

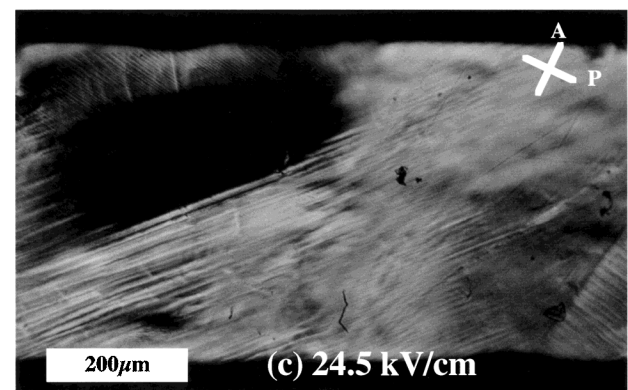
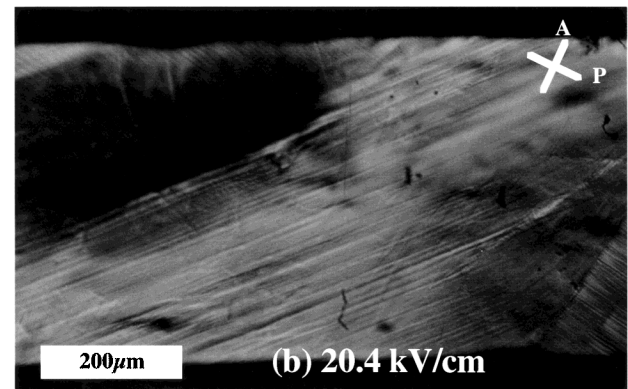
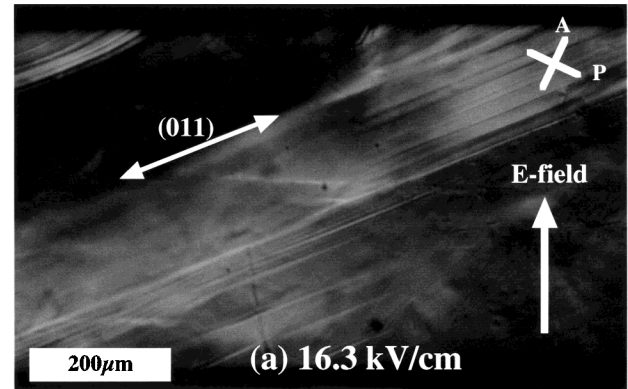


Fig. 10. *In situ* domain observation at various electric fields from 16.3 to 24.5 kV/cm in [111] oriented BaTiO₃ crystal.

in situ domain observation was done under electric fields from 25 to 30 kV/cm. As a result, at 29 kV/cm, small cracks occurred near the electrodes, and the cracks grew with increasing electric field. At 30 kV/cm, some regions with the extinction position along the [111] direction appeared partially, and then the crystal broke. This indicates the appearance of regions with polar direction of [111] at 30 kV/cm, *i.e.*, the formation of rhombohedral $3m$ phase in monoclinic *m* BaTiO₃ crystals. Details on this are also described elsewhere.¹⁴⁾ As shown in Fig. 6, above 40 kV/cm, there is no hysteresis, which suggests the formation of single-domain state in rhombohedral BaTiO₃ crystals. Therefore, we consider that in the electric-field region from 30 to 40 kV/cm, two phases, monoclinic *m* and rhombohedral $3m$, coexisted, and above 40 kV/cm, all of regions became to rhombohedral $3m$ phase. The above results reveal that above 30 kV/cm, an

electric-field-induced phase transition occurred from monoclinic to rhombohedral phase, and thus resulted in the discontinuous change and large hysteresis as shown in Fig. 6. Moreover, in single-domain rhombohedral BaTiO₃ crystals over 40 kV/cm, the apparent d_{33} was around 145 pC/N, which was 1.2 times larger than that in [001] poled single-domain tetragonal BaTiO₃ crystals. This difference is also discussed elsewhere.¹⁴⁾

4. Conclusions

In BaTiO₃ single crystals, piezoelectric properties were investigated at room temperature as a function of the crystal crystallographic orientation. When a unipolar electric field was applied along the [001] direction, the strain *vs* electric-field curve showed a large hysteresis, and finally BaTiO₃ crystal became to single-domain state with d_{33} of 125 pC/N over 20 kV/cm. *In situ* domain observation revealed that this large hysteresis is caused by a difference in domain wall density at increase and decrease of electric fields. On the other hand, the strain *vs* electric-field curve in [111] oriented BaTiO₃ single crystals exhibited a very complicated strain behavior. An electric-field exposure below 6 kV/cm along the [111] direction resulted in a high d_{33} of 203 pC/N and a non-hysteretic strain *vs* electric-field behavior, which suggested the formation of the engineered domain configuration in a tetragonal BaTiO₃ crystal. Therefore, it was confirmed that application of the engineered domain configuration to tetragonal BaTiO₃ crystals caused more enhanced piezoelectric activities compared with single-domain BaTiO₃ crystals. Moreover, when electric field over 6 kV/cm were applied along the [111] direction, two discontinuous changes at around 10 and 30 kV/cm were observed in the strain *vs* electric-field curve. *In situ* domain observation and *in situ* Raman measurement under electric fields suggested that the discontinuous change around 10 kV/cm can be assigned to the electric-field-induced phase transition from **4mm** to **m** while the discontinuous change around 30 kV/cm was assigned to the electric-field-induced phase transition from **m** to **3m**. Moreover, in monoclinic BaTiO₃ crystal, an electric-field exposure from 16 to 26 kV/cm along the [111] direction gave a high d_{33} of 295 pC/N and a hysteresis-free strain *vs* electric-field behavior, which revealed the formation of another new engineered domain configuration in a monoclinic BaTiO₃ crystal. In this study, we found two engineered domain configurations in the [111] poled **4mm** and **m** BaTiO₃ single crystals and their

enhanced piezoelectric properties. The difference in d_{33} between tetragonal and monoclinic phases with different engineered domain configurations will be discussed on the basis of crystallography elsewhere.¹⁴⁾ On the basis of the above results, we believe that the concept of the engineered domain configuration is universal and can be applied to all perovskite-type ferroelectric crystals, and improved piezoelectric activity can be achieved.

Acknowledgements

We would like to thank Dr. A. Kurosaka and Mr. O. Nakao of Fujikura, Ltd. for preparing TSSG-grown BaTiO₃ single crystals with excellent chemical quality. This study was partially supported by a Grant-in-Aid for Scientific Research (11555164) from the Ministry of Education, Science, Sports and Culture, Japan.

- 1) S.-E. Park, M. L. Mulvihill, P. D. Lopath, M. Zipparo and T. R. Shrout: Proc. 10th IEEE Int. Symp. Applications of Ferroelectrics (1996) Vol. 1, p. 79.
- 2) S.-E. Park and T. R. Shrout: IEEE Trans. Ultrason. Ferroelectr. & Freq. Control **44** (1997) 1140.
- 3) S.-E. Park and T. R. Shrout: Mater. Res. Innovat. **1** (1997) 20.
- 4) S.-E. Park and T. R. Shrout: J. Appl. Phys. **82** (1997) 1804.
- 5) J. Kuwata, K. Uchino and S. Nomura: Ferroelectrics **37** (1981) 579.
- 6) J. Kuwata, K. Uchino and S. Nomura: Jpn. J. Appl. Phys. **21** (1982) 1298.
- 7) S. Wada, S.-E. Park, L. E. Cross and T. R. Shrout: J. Korean Phys. Soc. **32** (1998) S1290.
- 8) S. Wada, S.-E. Park, L. E. Cross and T. R. Shrout: Ferroelectrics **221** (1999) 147.
- 9) A. Kurosaka, K. Tomomatu, O. Nakao, S. Ajimura, H. Tominaga and H. Osanai: J. Soc. Mater. Eng. Res. **5** (1992) 74 [in Japanese].
- 10) S. Ajimura, K. Tomomatu, O. Nakao, A. Kurosaka, H. Tominaga and O. Fukuda: J. Opt. Soc. Am. B **9** (1992) 1609.
- 11) O. Nakao, K. Tomomatsu, S. Ajimura, A. Kurosaka and H. Tominaga: Jpn. J. Appl. Phys. **31** (1992) 3117.
- 12) O. Nakao, K. Tomomatsu, S. Ajimura, A. Kurosaka and H. Tominaga: Ferroelectrics **156** (1994) 135.
- 13) D.-S. Paik, S.-E. Park, S. Wada, S.-F. Liu and T. R. Shrout: J. Appl. Phys. **85** (1999) 1080.
- 14) S. Wada, S. Suzuki, T. Noma, T. Suzuki, M. Osada, M. Kakihana, S.-E. Park, L. E. Cross and T. R. Shrout: submitted to J. Appl. Phys.
- 15) M. Zgonik, P. Bernasconi, M. Duelli, R. Schlessler, P. Gunter, M. H. Garrett, D. Rytz, Y. Zhu and X. Wu: Phys. Rev. B **50** (1994) 5941.
- 16) J. Fousek: Czech. J. Phys. **B21** (1971) 955.
- 17) E. E. Wahlstrom: *Optical Crystallography* (John Wiley and Sons, New York, 1979) 5th ed., Chap. 10.
- 18) W. Merz: Phys. Rev. **91** (1953) 513.